

## **Supporting information**

### **Understanding Improved Electrochemical Properties of NiO-doped NiF<sub>2</sub>/C Composite Conversion Materials by X-ray Absorption Spectroscopy and Pair Distribution Function Analysis**

**Dae Hoe Lee<sup>a</sup>, Kyler J. Carroll<sup>a</sup>, Karena W. Chapman<sup>b</sup>, Olaf J. Borkiewicz<sup>b</sup>, Scott Calvin<sup>c</sup>,  
Eric E. Fullerton<sup>a</sup>, Ying Shirley Meng<sup>a</sup>**

*<sup>a</sup>Department of NanoEngineering, University of California San Diego, 9500 Gilman Drive,*

*La Jolla, CA 92093, USA*

*<sup>b</sup>X-ray Science Division, Advanced Photon Source, Argonne National Laboratory, 9700 South  
Cass Avenue, Argonne, IL 60439, USA*

*<sup>c</sup>Department of Physics, Sarah Lawrence College, Bronxville, NY 10708, USA*

Table S1. Parameters and reliability factors obtained by the Rietveld refinement of pure NiF<sub>2</sub>, NiO-NiF<sub>2</sub> and NiO-NiF<sub>2</sub>/C XRD patterns.

NiF <sub>2</sub> Space group: <i>P4<sub>2</sub>/mnm</i>						NiO-NiF <sub>2</sub> NiF <sub>2</sub> Space group: <i>P4<sub>2</sub>/mnm</i>						NiO-NiF <sub>2</sub> /C NiF <sub>2</sub> Space group: <i>P4<sub>2</sub>/mnm</i>					
Atom	Site	x	Y	z	Occ.	Atom	Site	x	y	z	Occ.	Atom	Site	x	Y	z	Occ.
Ni	2a	0	0	0	1	Ni	2a	0	0	0	1	Ni	2a	0	0	0	1
F	4f	0.298	0.298	0	2	F	4f	0.300	0.300	0	2	F	4f	0.298	0.298	0	2
a = b = 4.6675(6) Å, c = 3.0632(9) Å R <sub>wp</sub> = 2.26%, R <sub>B</sub> = 7.14%						a = b = 4.6421(5) Å, c = 3.0667(2) Å R <sub>wp</sub> = 2.39%, R <sub>B</sub> = 5.61%						a = b = 4.6354(2) Å, c = 3.0580(7) Å R <sub>wp</sub> = 3.66%, R <sub>B</sub> = 19.50%					
						NiO Space group: <i>Fm-3m</i>					NiO Space group: <i>Fm-3m</i>						
Atom	Site	x	y	z	Occ.	Atom	Site	x	Y	z	Occ.	Atom	Site	x	Y	z	Occ.
Ni	4a	0	0	0	1	Ni	4a	0	0	0	1	Ni	4a	0	0	0	1
O	4b	0.5	0.5	0.5	1	O	4b	0.5	0.5	0.5	1	O	4b	0.5	0.5	0.5	1
						a = b = c = 4.1648(9) Å R <sub>wp</sub> = 2.39%, R <sub>B</sub> = 7.19%					a = b = c = 4.1529(3) Å R <sub>wp</sub> = 3.66%, R <sub>B</sub> = 1.58%						

Table S2. The comparison of the amount of conversion reaction calculated by the electrochemical data and the linear combination fit of XANES.

	1 <sup>st</sup> discharge (%)		1 <sup>st</sup> charge (%)		2 <sup>nd</sup> discharge (%)	
	NiF <sub>2</sub>	NiO-NiF <sub>2</sub> /C	NiF <sub>2</sub>	NiO-NiF <sub>2</sub> /C	NiF <sub>2</sub>	NiO-NiF <sub>2</sub> /C
Electrochemical data	128	109	64	91	89	104
XANES	94.6	86.6	47	79.8	89.9	84.8

It is worth to note that the amount of side reaction such as SEI formation affects the electrochemical data significantly resulting in the differences in conversion amount calculated by XANES. For example, the conversion is higher than 100% in pure NiF<sub>2</sub> electrode due to the side reactions. However, the tendency of conversion amount is very similar in both methods.

Figure S1. The cycling performances of 4 different systems, pure  $\text{NiF}_2$ ,  $\text{NiF}_2/\text{C}$ ,  $\text{NiO-NiF}_2$ , and  $\text{NiO-NiF}_2/\text{C}$ , at room temperature. Constant current of  $C/20$  was applied, and the voltage range was 1.0 ~ 4.5 V.

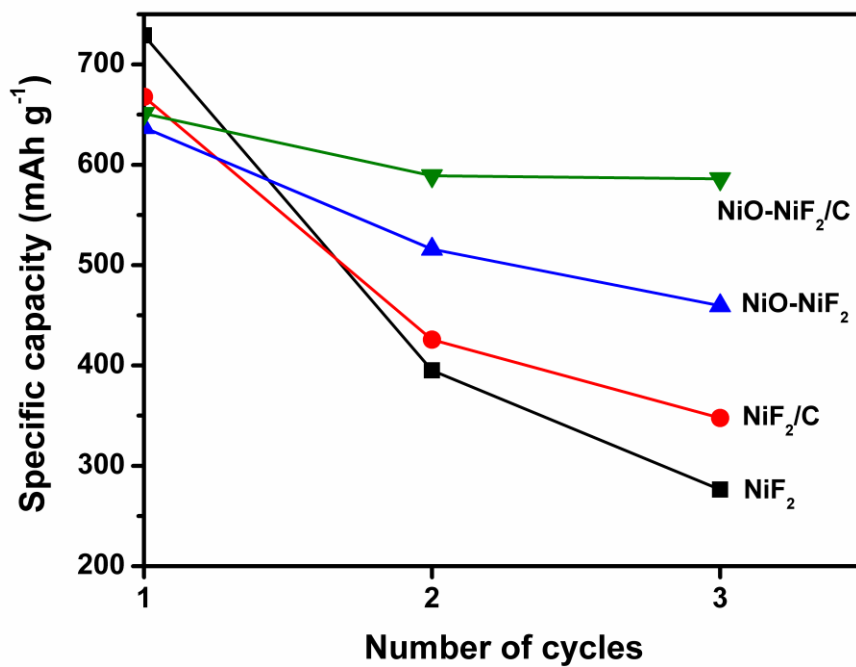


Figure S2. The electrochemical profiles of pure  $\text{NiF}_2$  at room temperature and  $70^\circ\text{C}$ . Constant current of  $C/20$  was utilized, and the voltage ranges were  $1.0 \sim 4.5$  V for the room temperature and  $1.5 \sim 4.5$  V for the elevated temperature cycling.

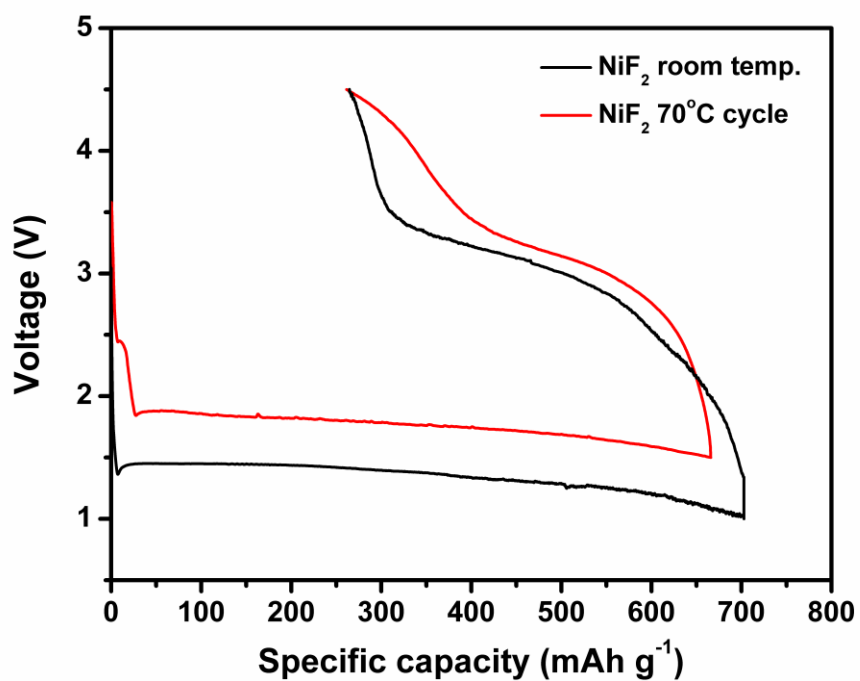


Figure S3. The 1<sup>st</sup> derivatives of XANES spectra of NiO-NiF<sub>2</sub>/C at initial, 1<sup>st</sup> discharged, 1<sup>st</sup> charged and 2<sup>nd</sup> discharged state. It is clearly observed that the energy shifts from 8345 eV (Ni<sup>2+</sup>) to 8333 eV (Ni<sup>0</sup>) upon the discharge and moved back to 8345 eV after the charge.

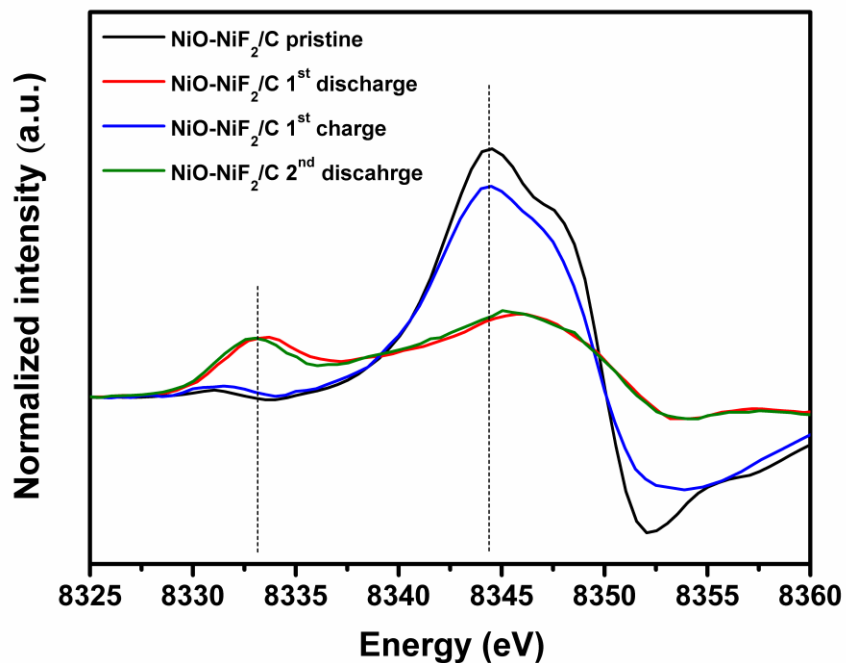


Figure S4. Experimental  $k^3$ -weighted  $\chi(k)$  plots for 1<sup>st</sup> and 2<sup>nd</sup> discharged NiO-NiF<sub>2</sub>/C and Ni foil as a reference (black dots).

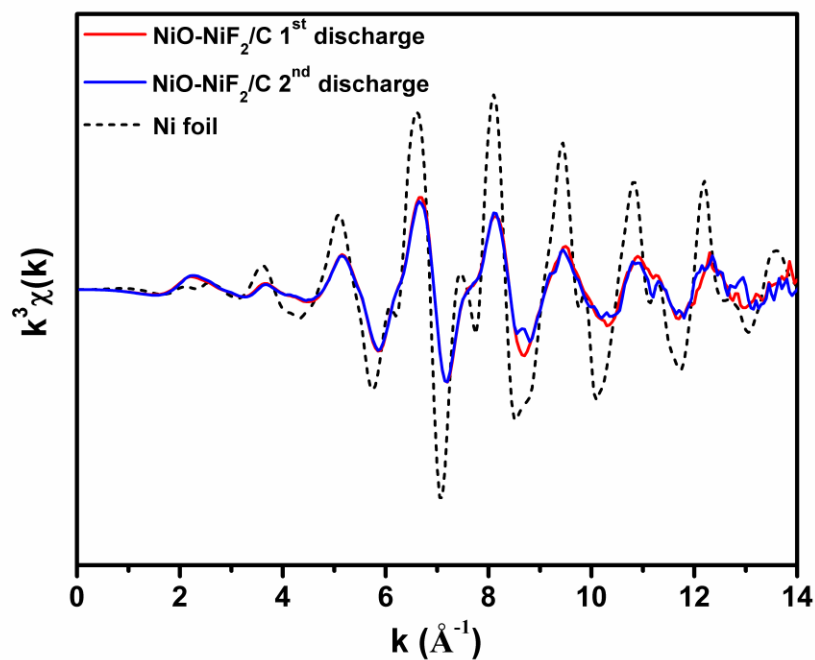


Figure S5. Experimental Fourier transformed  $k^3$ -weighted  $\chi(k)$  plot and fits for NiF<sub>2</sub> at (a) 1<sup>st</sup> and (b) 2<sup>nd</sup> discharged states, and NiO-NiF<sub>2</sub>/C at (c) 1<sup>st</sup> and (d) 2<sup>nd</sup> discharged states. R-factors are included in each figure.

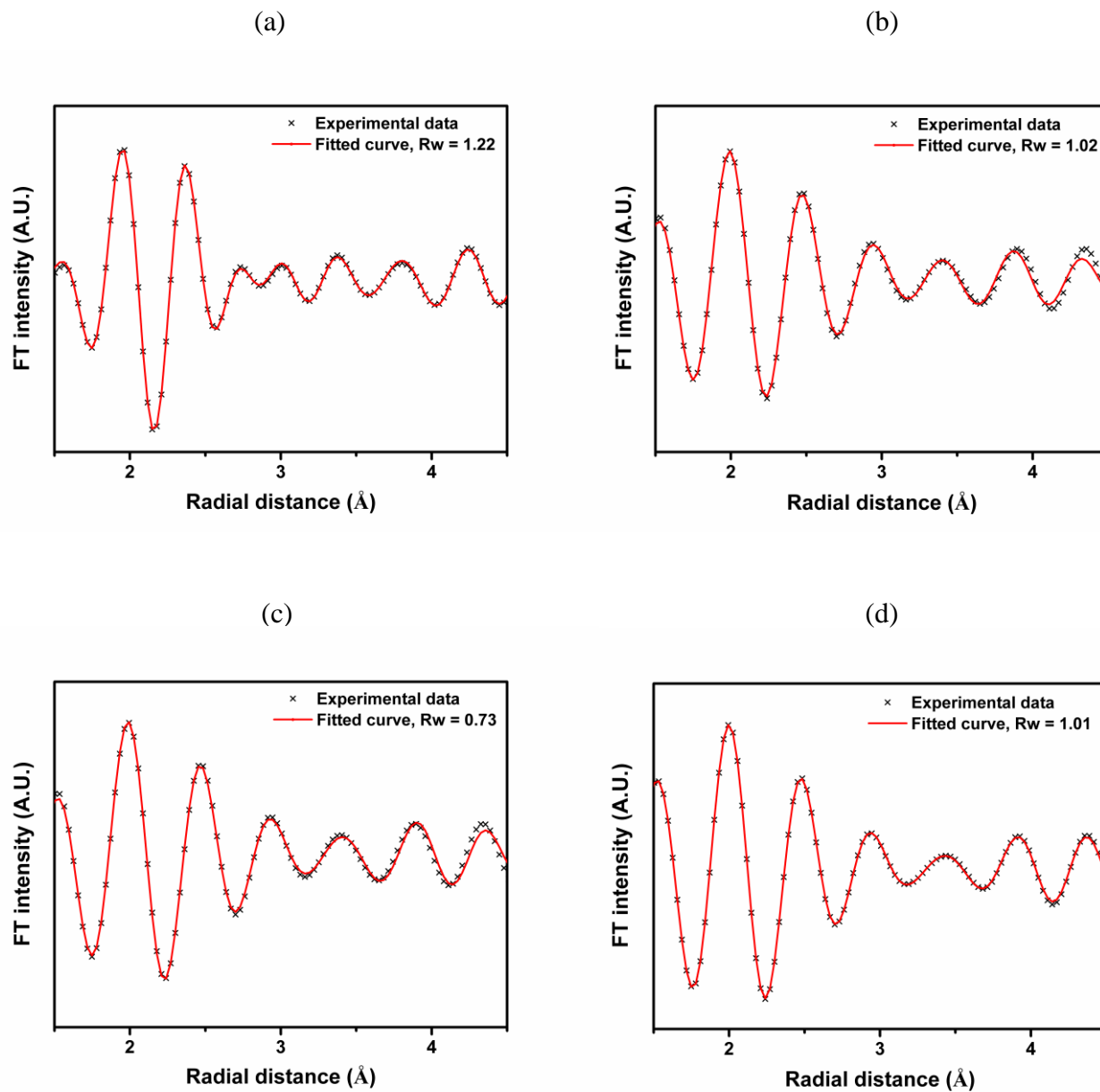


Figure S6. Experimental PDF,  $G(r)$ , profiles including refined fits and differences. (a)  $\text{NiF}_2$  1<sup>st</sup> discharge, (b)  $\text{NiF}_2$  2<sup>nd</sup> discharge, (c)  $\text{NiO-NiF}_2/\text{C}$  1<sup>st</sup> discharge and (d)  $\text{NiO-NiF}_2/\text{C}$  2<sup>nd</sup> discharge.

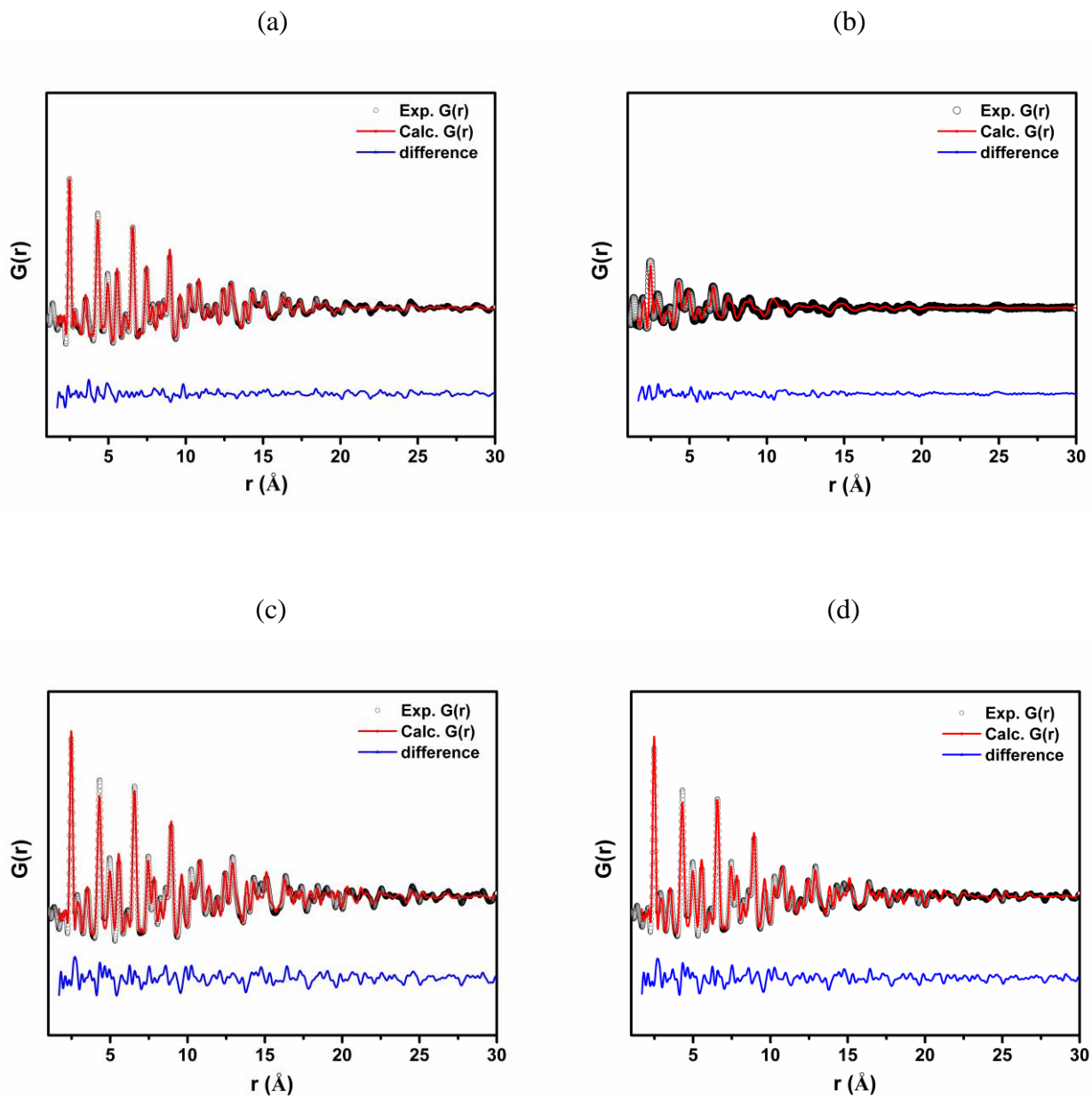


Figure S7. The schematics illustrating the conversion mechanisms in  $\text{NiF}_2$  and  $\text{NiO-NiF}_2/\text{C}$  at the 1<sup>st</sup> and 2<sup>nd</sup> discharge.

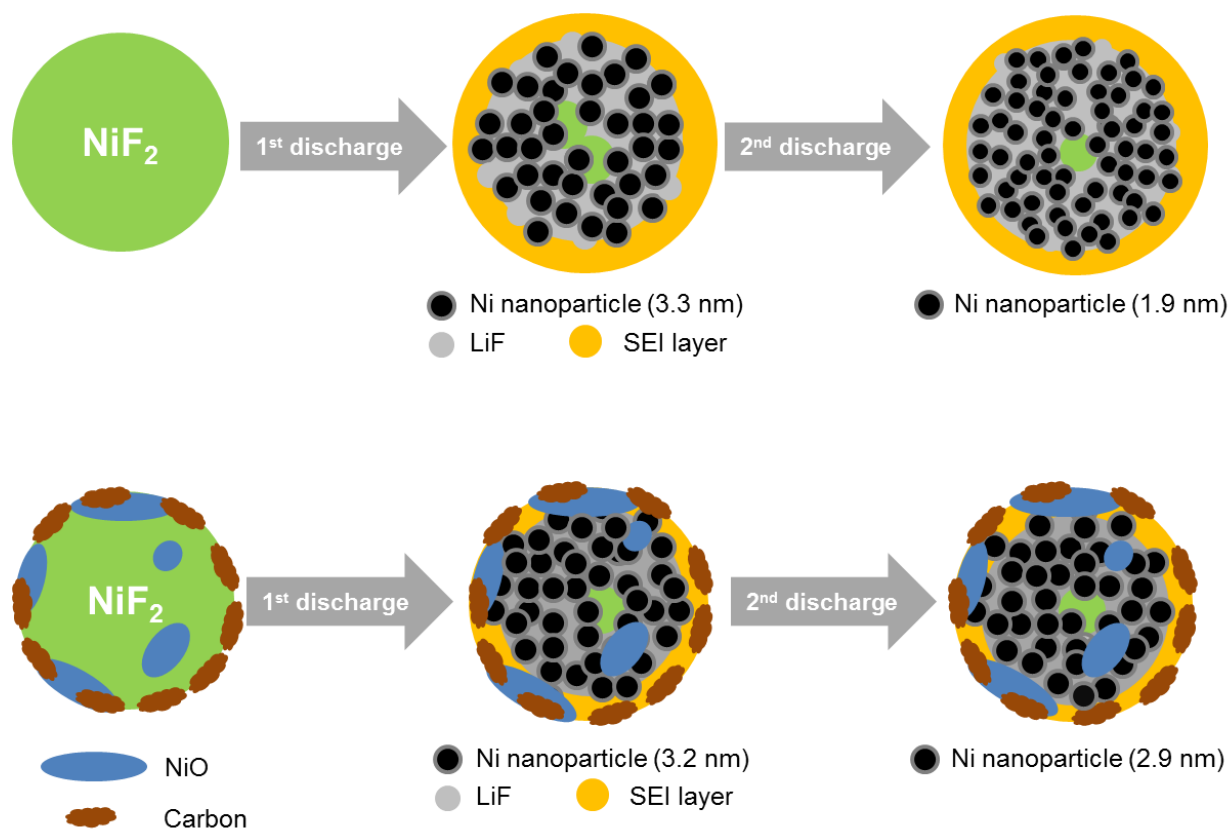
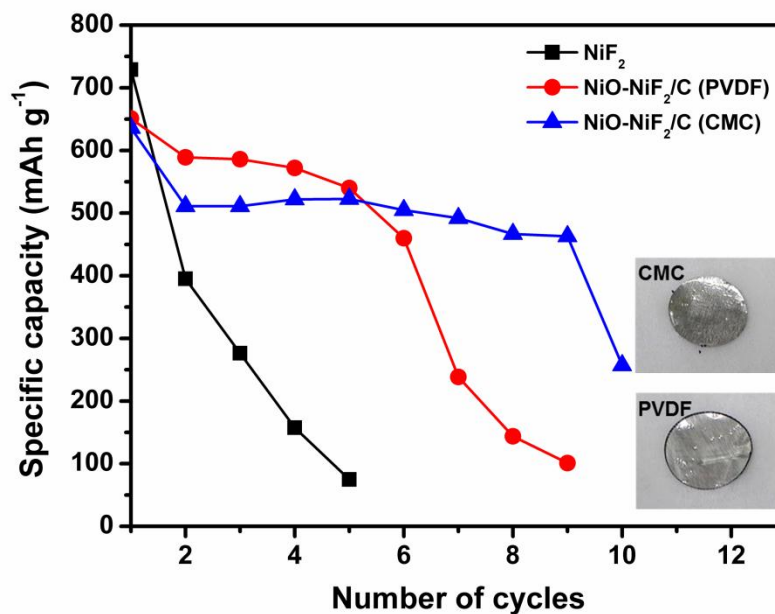


Figure S8. The electrochemical cycling properties of NiF<sub>2</sub> (black), and NiO-NiF<sub>2</sub>/C with PVDF (red) and CMC (blue) binder systems at C/20 rate at room temperature, and pictures of the cycled electrodes (insets).



CMC binder systems were utilized to improve the capacity retention of volume expanding conversion materials. CMC shows the extended conformation in the solution, which facilitates an efficient networking process between the conductive agent and active materials. In addition, the chemical bonding between CMC binder and the active material particles contributes to the enhanced capacity retention suppressing the volume expansion.<sup>1, 2</sup> Significantly improved cycling properties were observed in NiO-NiF<sub>2</sub>/C with CMC binder until 9<sup>th</sup> cycle. Except for the large irreversible capacity at the 1<sup>st</sup> cycle, 91% of capacity was retained from the 2<sup>nd</sup> to 9<sup>th</sup> cycle. Obvious volume expansion was found in the PVDF electrodes after the cycling (see Figure 6. (insets)). Although the theoretical volume expansion is 24% in the NiF<sub>2</sub> material, no remarkable

volume expansion was detected in CMC binder system. The chemical bonding between CMC and active materials possibly suppresses the volume changes maintaining the electronic contact with Al substrate. The capacity, however, was abruptly faded at the 10<sup>th</sup> cycle in CMC system. It is speculated that the pulverization of the electrode may cause the loss of the cathode materials from the electrode leading to considerable amount of capacity fading.

## References

1. J. Li, R. B. Lewis and J. R. Dahn, *Electrochem. Solid State Lett.*, 2007, **10**, A17-A20.
2. J. Li, D.-B. Le, P. P. Ferguson and J. R. Dahn, *Electrochimica Acta*, 2010, **55**, 2991–2995.